Mechanistic Studies Comparing the Incorporation of (+) and (−) Isomers of 3TCTP by HIV-1 Reverse Transcriptase†

Joy Y. Feng and Karen S. Anderson*

Department of Pharmacology, Yale University School of Medicine, 333 Cedar Street, New Haven, Connecticut 06520-8066

Received September 30, 1998; Revised Manuscript Received November 6, 1998

ABSTRACT: Among the nucleoside inhibitors used clinically as anti-HIV drugs which target HIV-1 reverse transcriptase (RT), (−)-2′,3′-dideoxy-3′-thiacytidine [(−)SddC or 3TC] is the only analogue with the unnatural L(−) nucleoside configuration. 3TC has been shown to be more potent and less toxic than the D(+) isomer, (+)SddC, which has the natural nucleoside configuration. The mechanistic basis for the stereochemical selectivity and differential toxicity of the isomeric SddC compounds is not completely understood although a number of factors may clearly come into play including differences in uptake, metabolic activation, degradation, and transport. We used a pre-steady-state kinetic analysis to determine the maximum rate of incorporation, k_{pol}, nucleotide-binding affinity, K_d, and efficiency of incorporation, k_{pol}/K_d, for the (−) and (+) isomeric SddCTP compounds as well as the corresponding dideoxy and natural nucleoside triphosphates into a primer−template complex using HIV-1 reverse transcriptase. The affinity (K_d) of the dNTP was much tighter and the efficiency (k_{pol}/K_d) of incorporation by enzyme into the primer−template complex was much higher for the DNA/RNA primer−template compared to DNA/DNA. The maximum rate of incorporation, k_{pol}, followed the trend of dCTP > ddCTP > (+)SddCTP > (−)SddCTP while the K_d values determined for the DNA/RNA primer−template followed the order (−)SddCTP ≅ (+)SddCTP ≅ ddCTP > dCTP. The corresponding efficiency of incorporation followed the trend dCTP > ddCTP > (+)SddCTP > (−)SddCTP. These data suggest that perturbations on the ribose ring of cytidine analogues (C → S) decrease the rate and efficiency of incorporation but enhance the binding affinity. These results are discussed in the context of a computer modeled structure of the ternary complexes of RT, DNA/RNA primer−template, and SddCTP analogues as well as implications for structure−activity relationships and further drug design. This information provides a mechanistic basis for understanding the inhibition of HIV-1 reverse transcriptase by 3TC.

Virally encoded reverse transcriptase (RT)[1] is required for replication of the human immunodeficiency virus (HIV), an etiological agent for acquired immunodeficiency syndrome (AIDS). RT has three catalytic activities that are essential for viral replication: RNA-dependent DNA polymerase, RNase H cleavage, and DNA-dependent DNA polymerase. RT is considered to be the molecular target of several therapeutic agents that interfere with HIV replication, including the 5′-*O*-triphosphates of 3′-azido-3′-deoxythymidine (AZT), 2′,3′-didehydro-2′,3′-dideoxythymidine(d4T), 2′,3′-dideoxycytidine (ddC), and the β-L-(−)-2′,3′-dideoxy-3′-thiacytidine [3TC, (−)SddC]. Among all of the nucleoside inhibitors currently used clinically, 3TC is the only one with the unnatural L-configuration. Most interestingly, 3TC and its corresponding 5-fluorinated derivative, (−)FTC, have been shown to be more potent and less toxic than the D-isomers (*1*−*4*). The mechanistic basis for the stereochemical selectivity and differential toxicity of the isomeric 3TC compounds is not completely understood although a number of factors may clearly come into play. The differences in potency and toxicity may be a combination of factors including uptake (*5*, *6*), transport (*7*), metabolic activation (*5*, *6*, *8*), incorporation (*5*, *6*, *8*, *9*), and degradation (*1*, *3*). In addition, toxicity to the host may also be related to inhibition of human mitochondrial DNA polymerase γ (*7*, *8*, *10*).

The mechanism of inhibition of HIV-1 RT by dideoxy nucleoside analogues such as 3TC [(−)SddC][2] involves in vivo phosphorylation to the triphosphate (3TCTP) and subsequent incorporation into the DNA primer strand resulting in chain termination. Thus in vitro studies have focused on evaluating the triphosphate form of the analogues. The steady-state kinetics for the (+) and (−)SddCTP analogue

† This work was supported by NIH Grant GM49551 to K.S.A.

* To whom correspondence should be addressed. Phone: 203-785-4526. E-mail: karen.anderson@yale.edu.

[1] Abbreviations: AIDS, acquired immunodeficiency syndrome; dCMP, 2′-deoxycytidine-5′-monophosphate; ddCMP, 2′,3′-deoxycytidine-5′-monophosphate; dCTP, 2′-deoxycytidine-5′-triphosphate; ddCTP, 2′,3′-deoxycytidine-5′-triphosphate; EDTA, (ethylenediamine)tetraacetate; HIV-1, human immunodeficiency virus type 1; RT, reverse transcriptase; (+)SddCMP, β-D-(+)-2′,3′-dideoxy-3′-thiacytidine-5′-monophosphate; (−)-SddCMP, β-L-(−)-2′,3′-dideoxy-3′-thiacytidine-5′-monophosphate; (+)SddCTP, β-D-(+)-2′,3′-dideoxy-3′-thiacytidine-5′-triphosphate; (−)SddCTP, β-L-(−)-2′, 3′-dideoxy-3′-thiacytidine-5′-triphosphate; 3TC, 2′,3′-dideoxy-3′-thiacytidine; 3TCMP, 2′,3′-dideoxy-3′-thiacytidine-5′-monophosphate; 3TCTP, 2′,3′-dideoxy-3′-thiacytidine-5′-triphosphate; (−)FTC, β-L-(−)-2′,3′-deoxy-5′-fluoro-3′-thiacytidine; Tris, tri(hydroxymethyl)aminomethane.

[2] The abbreviation 3TC is used to refer to the unnatural L or (−) isomer, (−)SddC. These are used interchangeably.

10.1021/bi982340r CCC: $18.00
Published on Web 12/15/1998

incorporation into DNA by HIV-1 RT has been studied (*6*, *8*, *11*). Steady-state kinetic analysis is important to provide an initial inhibitor evaluation; however, the analysis is limited by the fact that it reflects the rate-limiting step in the overall reaction pathway. On the other hand, a transient kinetic analysis allows one to examine each of the individual steps in the pathway including the identification of enzyme intermediates and conformational changes which might be associated with chemical catalysis. This is particularly true in considering the catalytic reaction pathway for RT. The reaction pathway is ordered, and the first step involves the binding of the DNA (or RNA) substrate to the enzyme to form a tight E−DNA complex with a K_d value in the nanomolar range. This step is followed by the binding of the correct nucleoside triphosphate. The enzyme checks for proper base-pairing geometry and then undergoes a rate-determining conformational change which limits chemical catalysis. The maximum rate of incorporation, k_{pol}, is governed by this conformational change. The slowest step in the pathway, k_{ss}, involves the dissociation of the elongated DNA substrate from the enzyme and is the step which is being examined in a steady-state kinetic analysis (*12*).

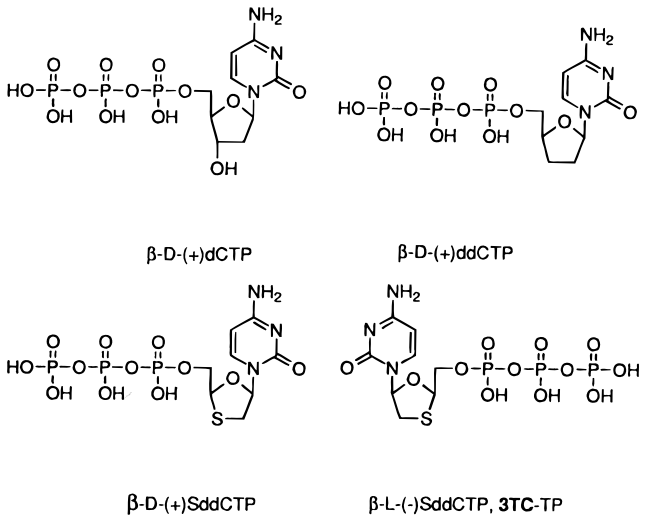

FIGURE 1: Structures of the 2′,3′-dideoxycytidine 5′-triphosphate analogues.

A recent pre-steady-state kinetic analysis has examined the (−) 3TCTP interaction with wild type and mutant forms of RT (*12*). In the present study, we used a transient kinetic approach to determine the k_{pol}, K_d, and efficiency of incorporation (k_{pol}/K_d) for dCTP, ddCTP, and the (+) and (−) 3TCTP isomers (Figure 1) using synthetic 23/45-mer DNA/RNA and DNA/DNA primer−templates (Figure 2).

DNA/DNA 23/45-mer:

```
*GCCTCGCAGCCGTCCAACCAACT
CGGAGCGTCGGCAGGTTGGTTGAGTTGGAGCTAGGTTACGGCAGG*
```

DNA/RNA 23/45-mer:

```
*GCCTCGCAGCCGTCCAACCAACT
CGGAGCGUCGGCAGGUUGGUUGAGUUGGAGCUAGGUUACGGCAGG*
```

FIGURE 2: Sequence of the oligonucleotide substrates. * Indicates 5′-[^{32}P] labeling of the oligomer.

Specific questions these studies were designed to address include the following: (1) Are there differences in incorporation into a DNA/RNA and DNA/DNA primer−template? (2) What are the kinetic and thermodynamic consequences of including a sulfur in the ribose ring? and (3) Does the stereochemistry of the nucleoside affect incorporation and RNase H cleavage? The results in this study provide a quantitative description of the interactions of these nucleoside triphosphates with DNA/RNA or DNA/DNA primer−template bound to RT and allow us to address kinetic and thermodynamic issues related to stereochemistry and isosteric replacement (C → S) in the ribose ring of cytidine analogues.

MATERIALS AND METHODS

Overexpression and Purification of HIV-1 RT. HIV-1 RT was purified as previously described (*13*, *14*). The protein concentration of purified RT was measured spectrophotometrically at 280 nm using an extinction coefficient ϵ_{280} = 260 450 M^{-1} cm^{-1}. The concentration of active RT was determined as previously described with pre-steady-state burst experiments (*13*) that gave burst amplitudes in the range 40−50%. The experiments described in the current study were performed using the corrected active site concentration.

Nucleotide Triphosphates and Other Materials. dCTP and ddCTP were purchased from Pharmacia LKB Biotechnology Inc. The (+)SddCTP and (−)SddCTP (3TCTP) were kindly provided by Dr. R. F. Schinazi (Emory University, Atlanta, GA). The purity of these compounds (>99%) was verified by HPLC analysis as well as LC/ESI mass spectrometry. [γ-^{32}P] ATP was purchased from Amersham. Biospin columns for the removal of excess nucleotide were purchased from Bio-Rad.

Synthetic Oligonucleotides. The DNA oligonucleotides (23- and 45-mer) shown in Figure 2 were synthesized on an Applied Biosystems 380A DNA synthesizer (DNA synthesis facility, Yale University) and purified using denaturing polyacrylamide gel electrophoresis (16% acrylamide, 8 M urea). The RNA oligonucleotide (45-mer, Figure 2) was synthesized and gel purified by New England Biolabs.

The duplex 23/45-mer primer−template of DNA/RNA and DNA/DNA was formed by annealing an approximately 1:1.3 molar ratio of pure 23- and 45-mer at 80 °C for 4 min and 50 °C for 30 min. The duplex mixtures were analyzed by nondenaturing polyacrylamide gel electrophoresis (15%) to ensure that proper annealing had taken place. Concentrations of the oligonucleotides were estimated by UV absorbance at 260 nm using the following calculated extinction coefficients: DNA 23-mer, ϵ = 226 750 M^{-1} cm^{-1}; DNA 45-mer, ϵ = 491 960 M^{-1} cm^{-1}; RNA 45-mer, ϵ = 507 960 M^{-1} cm^{-1}.

Buffers. All experiments using HIV-1 RT were carried out in 50 mM Tris-Cl, 50 mM NaCl buffer at pH 7.8 and at a temperature of 37 °C. All experimental procedures were carried out using sterile buffers, reagents, and glassware where feasible.

5′-^{32}P-Labeling of 23/45-mers. Before annealing both primer and template strands of the DNA/RNA and DNA/DNA 23/45-mer were 5′-radiolabeled with T4 polynucleotide kinase (New England Biolabs) according to previously described procedures (*13*).

Rapid-Quench Experiments. Rapid chemical quench experiments were performed as previously described with a

KinTek Instruments Model RQF-3 rapid-quench-flow apparatus (*13*, *14*). Unless noted otherwise, all concentrations refer to the final concentrations after mixing.

Pre-Steady-State Burst and Single-Turnover Experiments. A pre-steady-state kinetic analysis was used to examine the incorporation of next correct nucleotide into a DNA/RNA or DNA/DNA duplex at 37 °C. The analysis was conducted under the conditions in which the duplex concentration was three times greater than the enzyme concentration. The reaction was carried out by mixing a solution containing the preincubated complex of 100 nM HIV-1 RT and 5′-labeled 300 nM DNA/RNA or DNA/DNA duplex with a solution of 10 mM Mg^{2+} and varying concentrations of dNTP (in the range of 0.5 μM to 1 mM). Polymerization was quenched with 0.3 M EDTA at time intervals ranging from 3 ms to 3 min. DNA polymerization products and RNA cleavage products were quantified by sequencing gel analysis. The product formation occurred in a fast phase followed by a slow phase. The data were fitted to a burst equation (see Data Analysis). In examining the incorporation of (−)-SddCTP into a DNA/DNA primer−template, no pre-steady-state burst of product was observed (see Results). Although a pre-steady-state burst of product was observed for incorporation of (+)SddCTP into a DNA/DNA primer−template, the burst phase was rather shallow. Therefore single-turnover experiments were necessary in order to determine the K_d and k_{pol} values for incorporation of (−) and (+)SddCTP into a DNA/DNA primer−template. Single-turnover experiments were performed in a manner similar to that described above except that enzyme (400 nM) was used in excess of 5′-labeled DNA/DNA duplex (100 nM).

Product Analysis. The products were analyzed by sequencing gel electrophoresis (20% acrylamide, 8 M urea, 1 × TBE running buffer), and the products were quantified using a Bio-Rad GS525 Molecular Imager (Bio-Rad Laboratories, Inc., Hercules, CA).

Data Analysis. Data were fitted by nonlinear regression using the program KaleidaGraph version 3.09 (Synergy Software, Reading, PA). Data from burst experiments were fitted to a burst equation: $[\text{Product}] = A[1 - \exp(-k_{obsd}t) + k_{ss}t]$, where A represents the amplitude of the burst which correlates with the concentration of enzyme in active form, k_{obsd} is the observed first-order rate constant for dNTP incorporation, and k_{ss} is the observed steady-state rate constant. Data from single-turnover experiments were fit to a single exponential. The K_d, the dissociation constant of dNTP binding to the complex of RT and 23/45 duplex, is calculated by fitting the data to the following hyperbolic equation: $k_{obsd} = (k_{pol}[\text{dNTP}])/(K_d + [\text{dNTP}])$, where k_{pol} is the maximum rate of dNTP incorporation, [dNTP] is the corresponding concentration of dNTP, and K_d is the equilibrium dissociation constant for the interaction of dNTP with the E−DNA complex.

Computer Modeling. All molecular modeling of the enzyme complex was carried out on a Silicon Graphics Indigo[3] IMPACT workstation using INSIGHT II 95.0 software (Biosym/MSI, San Diego). The A-form DNA/RNA hybrid was constructed with the Build program within INSIGHT II. In our model, the dCTP and its three analogues were built using the Biosym Build program. The nucleosides (in the anti conformation) were first energy minimized and followed by addition of the triphosphate ester. The torsion angles of the triphosphate ester bonds were adjusted to −60°, 60°, or 180° to optimize the interaction with the catalytic aspartate triad without causing significant strain. The structures of the dNTPs obtained in this manner have similar overall shapes as compared to the ddCTP in the crystal structure of the ternary complex of DNA polymerase β and the ddGTP in the ternary complex of T7 DNA polymerase (*15*, *19*).The furanose conformation in our modeled dCTP, ddCTP is C2′-*exo*/C3′-*endo*, and the (+)SddCTP is C2′-*exo*/S3′-*endo*, all of which are consistent with the observed sugar pucker conformation in T7 DNA polymerase (*19*). For the analogue with unnatural L-configuration, the modeled (−)-SddCTP presented a similar S3′-*exo* envelope conformation in which the sulfur atom is out of the plane of the other atoms in the furanose ring. This is the conformation that is predicted from energy minimization, and it is consistent with that reported for the crystal structure of the nucleoside (−)-FTC, the 5-fluorinated analogue of (−)SddC (3TC) (*16*). The primer−template and dNTP were docked into RT according to the crystal structure studies with liganded HIV-1 RT, DNA polymerase β, and T7 DNA polymerase (*15*, *17*−*19*).

RESULTS

This study describes the kinetics of single-nucleotide incorporation of dCMP and its three analogues, ddCMP, (+)-SddCMP, and (−)SddCMP, opposite a template deoxyguanosine for DNA-dependent DNA polymerization and a template guanosine for RNA-dependent DNA polymerization with HIV-1 RT. Pre-steady-state burst and single-turnover experiments were conducted to determine the kinetic parameters for polymerization, k_{pol}, equilibrium dissociation constant, K_d, and incorporation efficiency, k_{pol}/K_d, for the dCTP analogue substrates (Figure 1), with defined homoduplex DNA/DNA 23/45-mer as well as analogous heteroduplex DNA/RNA 23/45-mer oligomer substrates (Figure 2). The pre-steady-state burst experiments also provided the linear steady-state rate, k_{ss}.

Incorporation of dNMP into a DNA/RNA or DNA/DNA 23/45-mer Primer −Template by HIV-1 RT. Pre-steady-state burst experiments were performed by mixing a preincubated solution of RT (100 nM) and 5′-[^{32}P]-labeled DNA/RNA 23/45-mer (300 nM) with Mg^{2+} (10 mM) and varying concentrations of dNTP under rapid-quench conditions. A representative time course for the incorporation of dCMP into the heteroduplex DNA/RNA 23/45-mer primer−template by HIV-1 RT is shown in Figure 3. A biphasic burst of product formation is observed. The solid line represents the best fit of the data to a burst equation with $k_{obsd} = 19 \pm 1\ s^{-1}$ and the observed $k_{ss} = 0.028 \pm 0.007\ s^{-1}$.

Analogous experiments were conducted with varying concentrations of dNTP [ddCTP, (+)SddCTP, or (−)-SddCTP] using both the heteroduplex (DNA/RNA) and homoduplex (DNA/DNA) primer−templates to examine the dNTP concentration dependence upon the observed burst rate k_{obsd} for each dNTP substrate. In experiments examining the incorporation of (−)SddCTP into the DNA/DNA primer−template no clear burst of product is observed indicating that the k_{pol} rate is similar or equal to the k_{ss}. These data imply

[3] The Tyr[115] and Phe[116] were treated as alanine due to poor or missing side chain electron density.

Table 1: Pre-Steady-State Kinetic Constants for dNTP Incorporation into D23/D45 and D23/R45

primer/template	dCTP analogues	k_{pol} (s^{-1})	K_d (μM)	k_{ss} (s^{-1})	k_{pol}/K_d (μM^{-1} s^{-1})
D23/D45	dCTP	1.9 ± 0.1	24 ± 5	0.04 ± 0.01	0.080
	ddCTP	0.35 ± 0.02	69 ± 11	0.05 ± 0.01	0.0051
	(+)SddCTP	0.036 ± 0.003	44 ± 9	0.007 ± 0.002	0.0008
	(−)SddCTP	0.019 ± 0.001	15 ± 3	0.015 ± 0.001	0.0013
D23/R45	dCTP	22.9 ± 0.7	30 ± 4	0.04 ± 0.01	0.76
	ddCTP	0.91 ± 0.04	5.3 ± 1.1	0.01 ± 0.001	0.17
	(+)SddCTP	0.10 ± 0.01	3.5 ± 0.4	0.004 ± 0.001	0.030
	(−)SddCTP	0.033 ± 0.002	5.0 ± 0.8	0.004 ± 0.001	0.0067

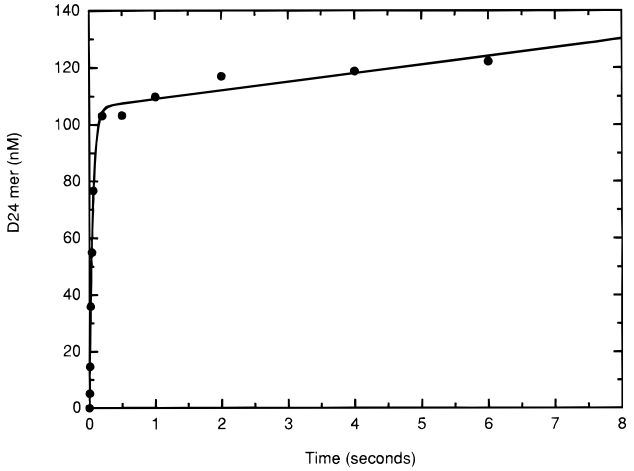

FIGURE 3: The pre-steady-state burst of dCTP. A preincubated 23/45 DNA/RNA heteroduplex (300 nM) with RT (100 nM active site concentration) was mixed with 150 μM dCTP in 10 mM Mg^{2+}-containing buffer to start the reaction. The reactions were quenched at the indicated time and analyzed by sequencing gel electrophoresis (20% acrylamide, 8 M urea). The solid line represents the fit to the burst equation as described, and the curves shown represent fits with $A = 106 \pm 2$ nM. The observed burst rate constant was 19 ± 1 s^{-1}, and the observed steady-state rate constant was 0.028 ± 0.007 s^{-1}.

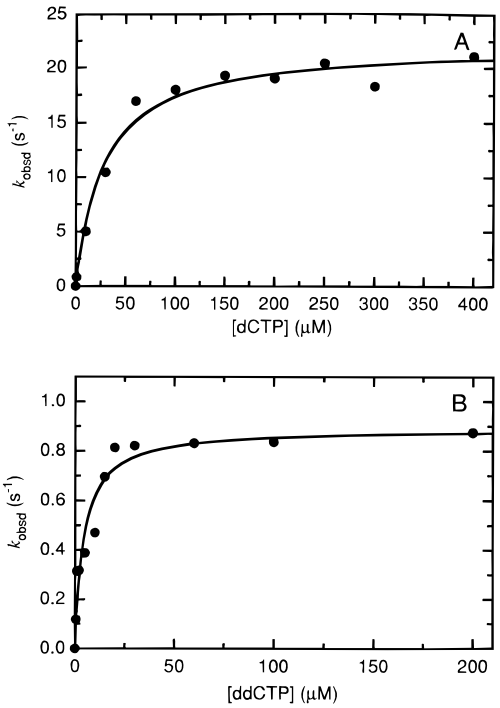

FIGURE 4: Dependence of the observed first-order rate k_{obsd} for dNTP incorporation on the concentration of dCTP and ddCTP. (A) The first-order rates against the dCTP concentrations. The observed rate was fit to a hyperbolic equation as described. The hyperbola (solid line) yielded a K_d value of 30 ± 4 μM for dCTP dissociation and a maximum rate of incorporation of 22.9 ± 0.7 s^{-1}. (B) The first-order rates against the ddCTP concentrations. The observed rate was fit to a hyperbola (solid line) which gave a K_d value of 5.3 ± 1.1 μM for ddCTP dissociation and a maximum rate of incorporation of 0.91 ± 0.04 s^{-1}.

that either the conformational change or chemistry may now represent the slowest step in the reaction pathway for incorporation of (−)SddCTP into a DNA/DNA primer−template. Since no burst of product was observed, single-turnover experiments with enzyme (400 nM) in excess over radiolabeled DNA/DNA 23/45-mer primer−template (100 nM) were used to determine the k_{pol} and K_d for (−)SddCTP. Although a burst of product was observed for incorporation of (+)SddCTP into a DNA/DNA primer−template, the burst phase was rather shallow; therefore single-turnover experiments were also used in this case to determine the k_{pol} and K_d for (+)SddCTP.

Determination of the Dissociation Constant for Nucleotide binding and Maximum Rates of Nucleotide Incorporation. The interaction of dCTP with the E−DNA complex was assessed by fitting the concentration dependence on the burst rates to the hyperbolic equation $k_{obsd} = (k_{pol}[dNTP]/(K_d + [dNTP])$, where k_{pol} is the maximum rate of dNTP incorporation, [dNTP] is the corresponding concentration of dCTP, and K_d is the equilibrium dissociation constant for the interaction of dCTP with the E−DNA complex. The concentration dependences of the observed polymerization rate for incorporation of dCTP and ddCTP into a DNA/RNA 23/45-mer primer−template using HIV-1 RT are shown in Figure 4, parts A and B, respectively.

The corresponding data for (+)SddCTP and (−)SddCTP are shown in Figure 5, parts A and B, respectively.

A complete summary of k_{pol}, K_d, and k_{pol}/K_d values for each dNTP with the DNA and RNA oligomer substrates is shown in Table 1.

A comparison of the analogues reveals that the natural substrate, dCTP, serves as the best substrate for RT. The maximum rate of dNTP incorporation, k_{pol}, was faster with a DNA/RNA primer−template, and in general, the affinity (K_d) was tighter, as compared with the DNA/DNA primer−template. In all cases the efficiency of incorporation was higher for RNA-dependent polymerization. An individual comparison of k_{pol} values for RNA-dependent polymerization indicates that dCTP is incorporated 25 times faster than the dideoxy analogue, while the (+) and (−) forms of SddCTP are incorporated at rates of 1/230 and 1/760, respectively, that of dCTP. For the DNA/DNA, ddCTP is incorporated 5-fold slower than dCTP but 10−18 times faster than the 3′-thio analogues. For both the DNA and RNA substrates, the (+)SddCTP isomer incorporates at a rate two to three times faster than the (−) isomer.

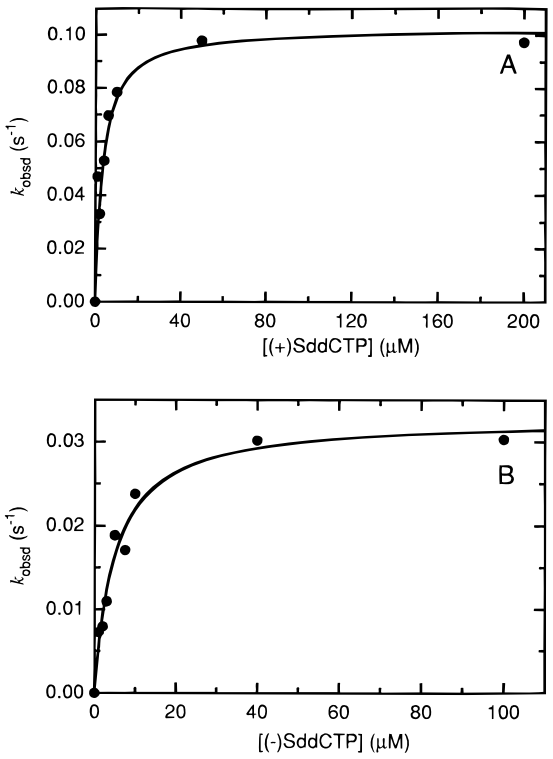

FIGURE 5: Dependence of the observed first-order rate constant k_{obsd} for dNTP incorporation on the concentration of (+)SddCTP and (−)SddCTP. (A) The first-order rates against the (+)SddCTP concentrations. The observed rate was fit to a hyperbolic equation as described. The hyperbola (solid line) yielded a K_d value of 3.5 ± 0.4 μM for (+)SddCTP dissociation and a maximum rate of incorporation of 0.10 ± 0.01 s^{-1}. (B) The first-order rates against the (−)SddCTP concentrations. The observed rate was fit to a hyperbola (solid line) which gave a K_d value of 5.0 ± 0.8 μM for ddCTP dissociation and a maximum rate of incorporation of 0.033 ± 0.002 s^{-1}.

The steady-state rate constants (k_{ss}) for the dNTPs which are obtained from the linear phase of the burst equation at saturating dNTP are summarized in Table 1. The efficiencies of incorporation (defined as k_{pol}/K_d), for dCTP, ddCTP, and (+) and (−)SddCTP are also listed in Table 1. For DNA/DNA homoduplex, the corresponding k_{pol}/K_d values for (+) and (−)SddCTP were quite similar. However, with a DNA/RNA heteroduplex, the value of k_{pol}/K_d for (+)SddCTP is greater than 4-fold higher than that of the (−) isomer. Taken together, these results indicate that the incorporation efficiency is much higher in RNA-dependent than in DNA-dependent polymerization.

Examination of RNase H Cleavage Activity. By simultaneous 5′-labeling of both the RNA template and DNA primer in the DNA/RNA 23/45 primer−template substrate, we could measure the relative rates of RNase H cleavage on the template strand as well as the pattern of RNA cleavage products which are formed. Previous studies in our lab have indicated that RNA cleavage is not influenced by the rate of polymerization, implying that the two catalytic activities are independent of one another (*13*, *14*). The length of the RNA cleavage products provides an indication of how the template strand is positioned between the polymerase and RNase H catalytic sites. Our previous studies have shown that there is a distance of approximately 19−21 oligonucleotide base pairs between the two active sites (*13*, *14*). In the present study, we examined the rate of RNase H cleavage as well as the RNA cleavage products formed with each of the cytidine analogues [dCTP, ddCTP, (+) and (−)SddCTP]. In addition, we also examined the corresponding (+) and (−) 5′-fluorinated SddCTP isomers (FSddCTP).

In contrast to the wide range of *polymerization* rates observed for the analogues (0.03−22.9 s^{-1}) there is little difference in the rates of RNase H cleavage (0.72−2.6 s^{-1}). In general the rate of cleavage was almost 2-fold faster for the natural (+) isomers of both SddCTP and FSddCTP as compared with the unnatural (−) isomers. A distinct pattern of RNA cleavage products was observed which was dependent upon whether the natural or unnatural isomers were bound as illustrated by the gel analysis shown in Figure 6.

The time course for simultaneous RNA cleavage and polymerization is shown in panels A, B, and C for dCTP, (+)SddCTP, and (−)SddCTP, respectively. For the natural forms of the dNTPs (dCTP and (+)SddCTP) two major cleavage products (a 41-mer and a 38-mer) were formed. Similar results were obtained with ddCTP and (+)FSddCTP (data not shown). The formation of a 41-mer RNase H cleavage product is consistent with a 19-nucleotide base pair difference between the polymerase and RNase H sites as previously determined (*13*, *14*). In contrast, for the unnatural isomers [(−)SddCTP and (−)FSddCTP], only one major product (a 41-mer) was observed. Although further work is required to more precisely define the nature of the RNA cleavage products, the data indicate that the RNA template may be positioned in a slightly different manner which is most likely influenced by the dNTP stereochemistry.

DISCUSSION

In this paper, we have examined the kinetics for the incorporation of dCMP, ddCMP, and (+)SddCMP and its unnatural β-L-(−) enantiomer, (−)SddCMP, into DNA/DNA and DNA/RNA primer−templates catalyzed by HIV-1 RT. Our studies have focused on understanding differences between DNA-dependent and RNA-dependent polymerization, the kinetic and thermodynamic consequences of including a sulfur in the ribose ring, and the effects of stereochemistry upon incorporation and RNase H cleavage.

Efficiency of Incorporation. A complete study of the dNTP concentration dependence on the burst rate of incorporation provided measurements for the dissociation constant, K_d, the maximum rate of dNMP incorporation, k_{pol}, and the efficiency of incorporation, k_{pol}/K_d. In agreement with the previous studies on dTMP incorporation using an analogous primer−template, the RNA-dependent incorporation is faster than the corresponding DNA-dependent polymerization (*13*, *14*). In this study, a more significant 12-fold difference between RNA-dependent and DNA-dependent polymerization was observed for dCMP incorporation, compared to 3−4-fold for incorporation of dTMP into a 25/45-mer. Correspondingly, all of the analogues were incorporated into an DNA/RNA primer−template much more efficiently. Our current findings are consistent with the previous steady-state studies (*8*).

DNA-Dependent Polymerization. When DNA serves as template, the maximum rate for dNMP incorporation followed the trend dCTP > ddCTP > (+)SddCTP and (−)-SddCTP. With a k_{pol} of 1.9 s^{-1}, dCTP was incorporated approximately 5 times faster than ddCTP, which in turn was

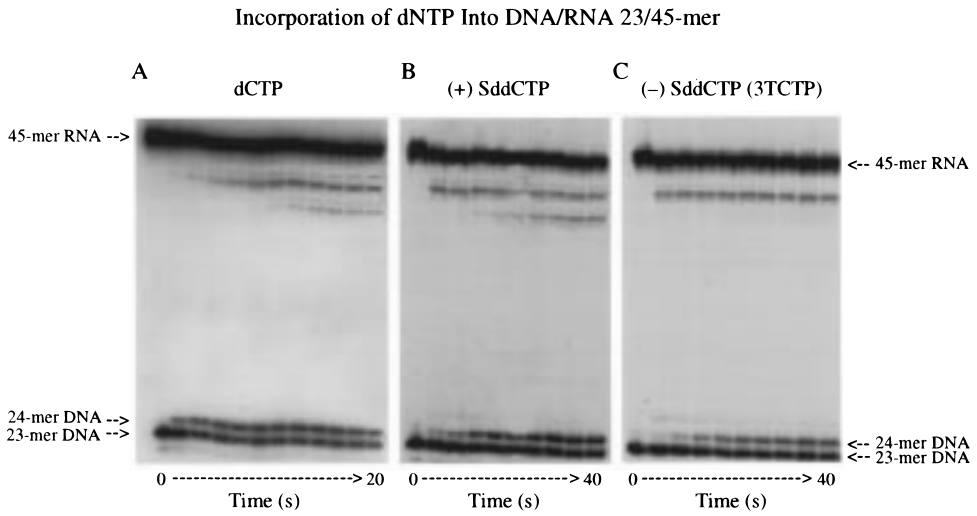

FIGURE 6: Gel analysis comparing the nature and kinetics of the RNase H cleavage activity in concert with the polymerization kinetics incorporating dCTP, (+)SddCTP, and (−)SddCTP. For each time course, a preincubated 23/45 DNA/RNA heteroduplex (300 nM) with RT (100 nM active site concentration) was mixed with a saturating concentration of dNTP in 10 mM Mg^{2+}-containing buffer to start the reaction. The reactions were quenched at the indicated time and analyzed by sequencing gel electrophoresis (20% acrylamide, 8 M urea) followed by phosphorimaging analysis. The sizes of the RNA template (45-mer), the DNA primer (23-mer), and the dNMP-extended product (24-mer) are indicated. It is clear from this analysis that the RNA cleavage products are different for the natural [dCTP and (+)SddCTP] and unnatural [(−)SddCTP] isomers.

10−20 times faster than the 3′-thio derivatives. However, the K_d values show that the binding affinity of these analogues is in the order (−)SddCTP ≥ dCTP > (+)SddCTP ≥ ddCTP. An examination of the relative efficiencies of incorporation (k_{pol}/K_d) revealed that ddCMP, (+)SddCMP, and (−)SddCMP were incorporated 10−50 times less efficiently than dCMP (Table 1). It is interesting to note that the (+) and (−)SddCTP were incorporated opposite a DNA template with similar efficiencies. Our data imply, however, that the rate-limiting step may have changed for the incorporation of the (−)SddCTP into a DNA/DNA primer−template since no burst of product was observed in a pre-steady-state burst experiment.

RNA-Dependent Polymerization. The analysis of RNA-dependent polymerization of the analogues indicated that, as the ribose ring was modified from 3′-OH of dCTP to 3′-deoxy in ddCTP to 3′-thio in the SddCTP isomers, the incorporation rate decreased remarkably. Previous transient kinetic studies have shown that there is a rate-limiting conformational change preceding chemical catalysis to form a tight enzyme−DNA−dNTP complex (*12*−*14*, *23*). Structural studies with several other DNA polymerases have confirmed the formation of the tight-fitting DNA−dNTP complex at the enzyme active site (*19*, *20*). Studies with other polymerases have suggested that the 3′-OH group of the ribose ring may affect catalysis directly through formation of an essential hydrogen bond with the enzyme that stabilizes substrate binding or indirectly by aiding in the alignment of the 5′-phosphate group in the active site (*23*, *24*). In the first case, we would predict that a missing 3′-OH group would have a dramatic effect on ground-state binding and accordingly, a weaker K_d value. Conversely, an indirect effect on alignment due to the lack of a 3′-OH would be expected to substantially decrease the rate of polymerization.

The binding affinity of dNTP to the RT−(DNA/RNA primer−template) complex is in the order (+)SddCTP ≥ (−)SddCTP ≥ ddCTP > dCTP, clearly showing that the K_d for the dideoxy analogues is actually tighter. However, the missing 3′-OH in ddCTP and the (+) and (−)SddCTP renders polymerization much slower. Therefore, our kinetic studies point to an indirect effect in which the 3′-OH group on the ribose ring is involved in poising the dNTP in a proper position for catalysis. Moreover, the presence of the more bulky sulfur atom in the ribose ring of the 3TCTP analogues most likely precludes the formation of a tight ternary complex, and thus, the analogues cannot fit as well as the natural substrate. The resulting perturbation of the ribose ring pucker may preclude the conformational change and hinder catalysis.

Although the unnatural (−)SddCTP analogue is incorporated more slowly than the natural substrate, dCTP, it binds to the enzyme−(DNA/RNA primer−template) complex with a 6-fold higher affinity than the dCTP. The tight binding of the (−)SddCTP may be one of the factors which contributes to the inhibitory efficiency observed with 3TC in cell culture which is comparable to that seen for AZT (*21*).

For all of the analogues, the incorporation efficiency is 5−40 times higher in RNA-dependent than in DNA-dependent polymerization. The order k_{pol}/K_d is dCTP > ddCTP > (+)SddCTP > (−)SddCTP. The K_d values obtained in this study reflect the true affinities of the dNTPs for the enzyme. Although larger, they are in general agreement with the K_m values previously reported from steady-state kinetic studies. The k_{ss} value for (−)SddCTP determined in this study is an order of magnitude faster than the steady-state k_{cat} values observed in earlier studies (*6*, *8*, *9*, *11*).

A Comparison of Enantiomers: Effects of Stereochemistry on Incorporation and RNase H Cleavage. The discovery that some L-nucleoside dideoxy analogues may be good inhibitors of polymerases such as HIV-1 RT and Hepatitis B viral polymerase (*5*, *25*) prompts some interesting mechanistic questions related to how the unnatural isomer may bind and be incorporated into a growing strand of DNA. In our current study, we were surprised to find that the maximum k_{pol} value was only 3-fold faster for the (+)SddCTP enantiomer as

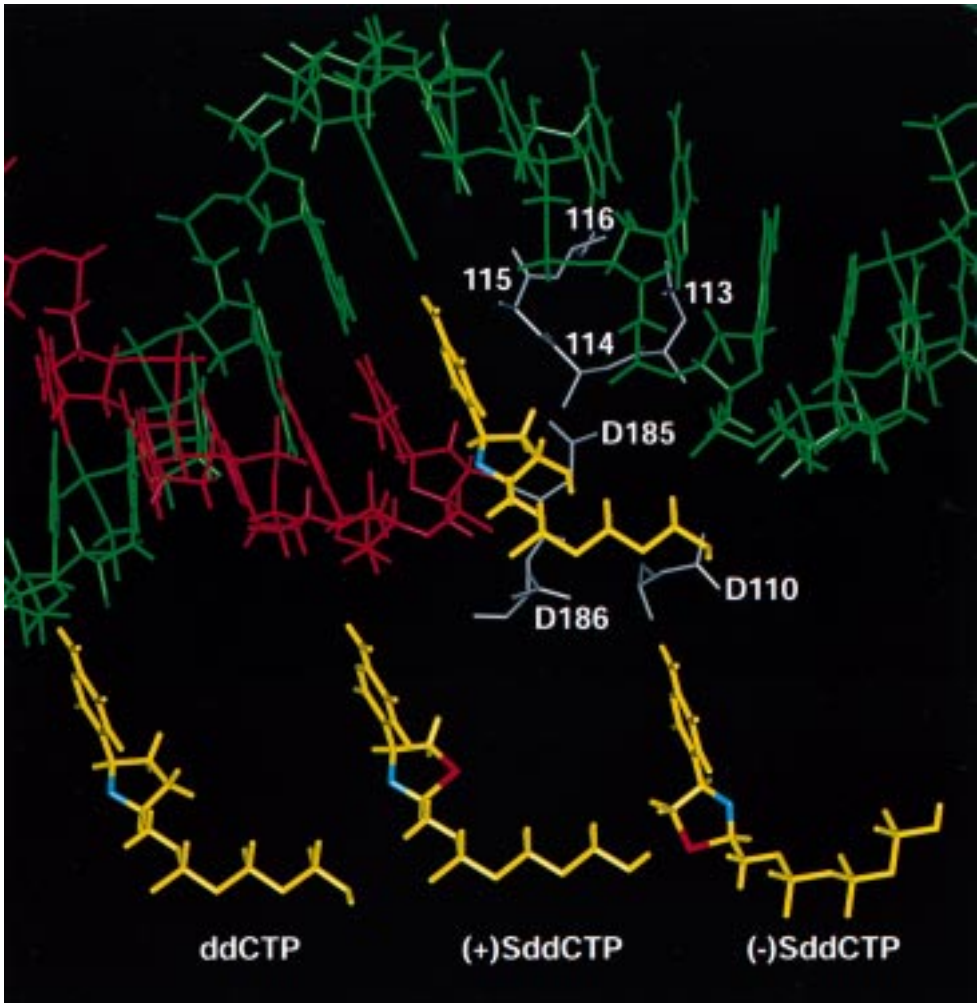

FIGURE 7: Structural representation showing the dCTP incorporation into DNA/RNA 23/45-mer primer (red)/template (green) at the HIV-1 RT polymerase catalytic site. For clarity, only part of carbon backbone of HIV-1 RT is shown in gray sticks. The catalytic triad (Asp^{110}, Asp^{185}, and Asp^{186}) and the suggested hydrophobic pocket (Asp^{113}, Ala^{114}, Try^{115}, and Phe^{116})[3] have close interaction with dCTP (shown in yellow, with ribose oxygen in blue). For comparison, the structures of the analogues are also shown with the ribose oxygen (blue) and the sulfur atom (red) highlighted.

compared with the (−)SddCTP. The efficiency of incorporation into a DNA/DNA primer−template for the (+)SddCTP analogue was similar to (−)SddCTP enantiomer, yet the (+)-SddCTP was incorporated into a DNA/RNA primer−template 4-fold more efficiently than the (−) isomer.

An ancillary issue is whether the RNase H activity is similar for each isomer. We found that the rate of RNase H cleavage for the unnatural isomer was approximately 2-fold slower than the natural one. Moreover, a different pattern of RNase H cleavage products was observed that was dependent upon whether a natural (dCTP, ddCTP, or (+)-SddCTP) or unnatural isomer [(−)SddCTP] was bound in the polymerase active site. The difference in the RNA cleavage products formed indicates that there are distinct variances in positioning the DNA/RNA primer−template−dNTP complex in the enzyme active site.

The biological activity of 3TC (unnatural isomer) and the corresponding (+) isomer have been studied from many different vantage points. It is important to keep in mind that 3TC or its (+) isomer must be phosphorylated by kinases to form the (−) and (+)SddCTP derivatives which are, in turn, incorporated into DNA by HIV-1 RT. In vitro studies using the triphosphate forms of the analogues have shown that the (+)SddCTP is more potent that the (−) isomer (*6*, *9*). However, in vivo cell culture studies have examined the effect of 3TC [(−)SddC] or (+)SddC and found the (−) isomer to have a similar or much higher potency dependent upon the cell line used (*2*, *3*, *26*). Moreover, the cellular toxicity appears to be greater for the (+)SddC; hence, it is the (−) isomer, 3TC, which is used clinically (*2*, *3*).

A number of factors are likely to contribute to the disparity between the in vitro and in vivo studies. While both isomers are substrates for cytosolic deoxycytidine kinase, only the (+)SddC is degraded by deoxycytidine deaminase (*1*, *3*). Thus the (+) isomer has a shorter half-life in cells (*1*, *3*). Moreover, removal of (+)-SddCMP-terminated-DNA is faster than the (−) isomer by a novel human cytosolic 3′-5′exonuclease (*6*). The cellular toxicity is considered to be primarily due to effects on the human mitochondrial DNA γ polymerase (*7*, *27*). The effects of the (+) and (−) isomers on the mitochondrial DNA γ polymerase are a function of their relative affinities (*9*, *10*), susceptibility of the SddCMP-terminated−DNA to removal by the exonuclease proofreading activity of the mitochondrial DNA γ polymerase (*8*), and stereoselective transport into the mitochondria by a novel mitochondrial transport protein (*5*).

Computer Modeling. We used computer modeling in an effort to understand, in structural terms, the stereochemical

effects on catalysis and how the natural and unnatural SddCTP isomers may bind at the active site. There is currently no published three-dimensional structure for the HIV-1 RT-DNA/RNA-dNTP complex (*17*, *18*; see also note added in proof). Therefore, we used the structural information available for HIV-1 RT as well as DNA polymerase β and T7 DNA polymerase to study the conformation of the DNA/RNA 23/45-mer (used in our kinetic studies) and the dCTP analogues bound at the polymerase active site of RT. While the presentative of any computer model of the RT−nucleic acid−dNTP complex is clearly speculative, we feel it is instructive for considering, in structural terms, how the natural and unnatural nucleotide triphosphates may be binding in the polymerase active site.

The conformation of the triphosphate ester was built according to the ddCTP in the crystal structure of DNA duplex-bound DNA polymerase β (*15*). Three major interactions are believed to influence the dCTP analogue conformation: (1) Watson−Crick base pairing between G and C; (2) chelation between the triphosphate ester and the aspartic acid triad (Asp^{110}, Asp^{185}, Asp^{186}) via coordination with Mg^{2+}; and (3) the interaction between the ribose ring and the loop between β6 and αC (including Asp^{113}) and portions of αC backbone (including Ala^{114}, Tyr^{115}, and Phe^{116}) (*15*).

A closeup view of our model at the polymerase active site is shown in Figure 7. The dCTP (shown in yellow, with ribose oxygen in blue) is base-paired with the DNA/RNA primer−template (shown in red and green). The structures of ddCTP, (+)SddCTP, and (−)SddCTP are shown below the active site in the figure, in a possible conformation plausible for base pairing and catalysis. The catalytic triad (Asp^{110}, Asp^{185}, and Asp^{186}) and a suggested hydrophobic pocket (Asp^{113}, Ala^{114}, Try^{115}, and Phe^{116})[3] are highlighted in gray. These residues are thought to have a close interaction with dCTP (shown in yellow, with ribose oxygen in blue). Mutagenesis studies suggest that Asp^{113}, while not essential for catalytic activity, may be involved in distinguishing normal nucleotide from ribose ring substituted analogues (*17*). In addition, point mutation studies indicate that three residues located in a hydrophobic pocket, Ala^{114}, Tyr^{115}, and Phe^{116}, may be involved in hydrophobic interactions with the incoming dNTPs (*17*).

Modeling of the natural D-configuration analogues [ddCTP and (+)SddCTP] indicates conformations similar to that adopted by the modeled structure of dCTP. However, to maintain proper base pairing, the L-configuration [(−)-SddCTP] must position the ribose ring in the opposite orientation, with the CH_2 and 3′-S atoms now pointing toward the 3′ end of the primer and the O atom pointing in the opposite direction. In this conformation, the 3′-sulfur in the ribose ring (shown in red) adopts a position similar to that of oxygen (shown in blue) in natural analogues. In this orientation, there are at least three structural features that may be important in governing binding and catalysis. First, electrostatic interactions in which the oxygen of the ribose ring acts as a hydrogen bond acceptor may be altered by substitution with sulfur. Second, the dihedral angle between the ribose ring and the α phosphate, which must be adopted for nucleophilic attack and catalysis by 3′-OH on the primer strand, may result in differences in the ring conformation and accommodation of the five-membered ring into the protein−primer−template complex. Third, the increased steric hindrance from the CH_2 and S atoms in the ribose ring substitution at 3′ position (C → S) may cause a distortion in the active site that interferes with the formation of the tight complex necessary for catalysis. Impeding the formation of this complex may significantly slow the rate of the conformational change and/or catalysis and subsequent (−)SddCMP incorporation.

Since the rate for (+)SddCMP incorporation is only 3-fold faster than that of the (−) isomer and almost 10-fold slower than the ddCTP, it is possible that the steric bulk of the ribose ring substitution at 3′(C → S) plays a more dominant role in governing catalysis than the stereochemistry. A definitive interpretation, in structural terms, must await the three-dimensional structures for the ternary complexes of each isomer and computational evaluations of the binding energetics.

Summary. The complete kinetic and thermodynamic analysis of dCTP, ddCTP, (+)SddCTP, and (−)SddCTP incorporation into RNA and DNA templates provides an in-depth, quantitative understanding of how each of these nucleotides interacts with HIV-1 RT. The structural modification on the ribose ring by introducing a sulfur atom leads to a perturbation which decreases the rate of incorporation but enhances the binding affinity of dNTP to HIV-1 RT. The relative differences between the (+) and (−) isomers is surprisingly small. Since we have shown that the efficiency of incorporation for 3TCTP (and (+)SddCTP) is much higher using a DNA/RNA primer−template than a DNA/DNA one, it is possible that inhibitory effects of 3TC are most important for RNA-dependent polymerization. The information gained from this study lays the necessary mechanistic groundwork for understanding inhibition and developing structure−activity relationships for related nucleoside analogues, and may aid in future drug design.

NOTE ADDED IN PROOF

The structure of the ternary complex of HIV-1 RT has recently been solved (*28*).

ACKNOWLEDGMENT

We thank Dr. Raymond Schinazi for the generous gift of (+) and (−)SddCTP and Dr. Stephen Hughes, Dr. Paul Boyer, and Dr. Andrea Ferris for the HIV-1 RT clone.

REFERENCES

1. Cammack, N., Rouse, P., Marr, C. L. P., Reid, P. J., Boehme, R. E., Coates, J. A. V., Penn, C. R., and Cameron, J. M. (1992) *Biochem. Pharmacol. 43*, 2059−2064.
2. Schinazi, R. F., McMillan, A., Cannon, D., Mathis, R., Lloyd, R. M., Peck, A., Sommadossi, J., St. Clair, M., Wilson, J., Furman, P. A., Painter, G., Choi, W. B., and Liotta, D. C. (1992) *Antimicrob. Agents Chemother. 36*, 2423−2431.
3. Chang, C. N., Doong, S. L., Zhou, J. H., Beach, J. W., Jeong, L. S., Chu, C. K., Tsai, C. H., and Cheng, Y. C. (1992) *J. Biol. Chem. 267*, 13938−13942.
4. Furman, P. A., Davis, M., Liotta, D. C., Paff, M., Frick, L. W., Nelson, D. J., Dornsife, R. E., Wurster, J. A., Wilson, L. J., Fyfe, J. A., Tuttle, J. V., Miller, W. H., Condreay, L., Averett, D. R., Schinazi, R. F., and Painter, L. (1992) *Antimicrob. Agents Chemother. 36*, 2686−2692.
5. Chang, C. N., Skalski, V., Zhou, J., and Cheng, Y. C. (1992) *J. Biol. Chem. 267*, 22414−22420.
6. Skalski, V., Chang, C. N., Dutschman, G., and Cheng, Y. C. (1993) *J. Biol. Chem. 268*, 23234−23238.

7. Parker, W. B., and Cheng, Y. C. (1994) *J. NIH Res. 6*, 57−60.
8. Gray, N. M., Marr, C. L., Pene, C. R., Cameron, J. M., and Bethell, R. C. (1995) *Biochem. Pharmacol. 50*, 1043−1051.
9. Hart, G. J., Orr, D. C., Penn, C. R., Figueiredo, H. T., Gary, N. M., Boehme, R. E., and Cameron, J. M. (1992) *Antimicrob. Agents Chemother. 36*, 1688−1694.
10. Kukhanova, M., Liu, S. H., Mozzherin, D., Lin, T. S., Chu, C. K., and Cheng, Y. C. (1995) *J. Biol. Chem. 270*, 23055−23059.
11. Ueno, T., and Mitsuya, H. (1997) *Biochemistry 36*, 1092−1099.
12. Krebs, R., Immendorfer, U., Thrall, S., Wohrl, B., and Goody, R. (1997) *Biochemistry 36*, 10292−10300.
13. Kati, W. M., Johnson, K. A., Jerva, L. F., and Anderson, K. S. (1992) *J. Biol. Chem. 36*, 25988−25997.
14. Kerr, S. G., and Anderson, K. S. (1997) *Biochemistry 36*, 14064−14070.
15. Pelletier, H., Sawaya, M. R., Kumar, A., Wilson, S. H., and Kraut J. (1994) *Science 264*, 1891−1903.
16. Van Roey, P., Pangborn, W. A., Schinazi, R. F., Painter, G., and Liotta, D. C. (1993) *Antiviral Chem. Chemother. 4*, 369−375.
17. Patel, P. H., Jacobo-Molina, A., Ding, J., Tantillo, C., Clark, A. D., Jr., Raag, R., Nanni, R. G., Hughes, S. H., and Arnold, E. (1995) *Biochemistry 34*, 5351−5363.
18. Kohlstaedt, L. A., Wang, J., Friedman, J. M., Rice, P. A., and Steitz, T. A. (1992) *Science, 256*, 1783−1790.
19. Doublié, S., Tabor, S., Long, A. M., Richardson, C. C., and Ellenberger, T. (1998) *Nature 391*, 251−258.
20. Kiefer, J. R., Mao, C., Braman, J. C., and Beese, L. S. (1998) *Nature 391*, 304−307.
21. Coates, J. A. V., Cammack, N., Jenkinson, H. J., Jowett, A. J., Jowett, M. I., Pearson, B. A., Penn, C. R., Rouse, P. L., Viner, K. C., and Cameron, J. M. (1992) *Antimicrob. Agents Chemother. 36*, 733−739.
22. Goody, R. S., Müller, B., and Restle, T. (1991) *FEBS Lett. 291*, 1−5.
23. Johnson, K. A. (1993) *Annu. Rev. Biochem. 62*, 685−713.
24. Brandis, J., Edwards, S., and Johnson, K. A. (1996) *Biochemistry 35*, 2189−2200.
25. Schinazi, R. F., Chu, C. K., Peck, A., McMillan, A., Mathis, R., Cannon, D., Jeong, L., Beach, J., Choi, W. B., Yeola, S., and Liotta, D. C. (1992) *Antimicrob. Agents Chemother. 36*, 672−76.
26. Coates, J. A. V., Cammack, N., Jenkinson, H. J., Mutton, I., Pearson, B. A., Storer, R., Cameron, J. M., and Penn, C. R. (1992) *Antimicrob. Agents Chemother. 36*, 202−205.
27. Martin, J. L., Brown, C., Matthews-Davis, N., and Reardon, J. (1994) *Antimicrob. Agents Chemother. 38*, 2743−2749.
28. Huang, H., Verdine, G. L., Chopra, R., and Harrison, S. C. (1998) *Science 282*, 1669.

BI982340R